



1

2 **Seasonal variability in methane and nitrous oxide fluxes from tropical peatlands in the**  
3 **Western Amazon basin**

4

5 Teh, Yit Arn<sup>1\*</sup>, Murphy, Wayne A.<sup>2</sup>, Berrio, Juan-Carlos<sup>2</sup>, Boom, Arnould<sup>2</sup>, and Page, Susan E.<sup>2</sup>

6 <sup>1</sup>Institute of Biological and Environmental Sciences, University of Aberdeen

7 <sup>2</sup> Department of Geography, University of Leicester

8 \* Author to whom all correspondence should be addressed; email: [yateh@abdn.ac.uk](mailto:yateh@abdn.ac.uk)



9     **2. ABSTRACT**

10    Here we report methane ( $\text{CH}_4$ ) and nitrous oxide ( $\text{N}_2\text{O}$ ) fluxes from lowland tropical peatlands  
11    in the Pastaza-Marañón foreland basin (PMFB) in Peru, one of the largest peatland complexes  
12    in the Amazon basin. Trace gas fluxes were sampled from the most numerically-dominant  
13    peatland vegetation types in the region: forested vegetation, forested (short pole) vegetation,  
14    *Mauritia flexuosa*-dominated palm swamp, and mixed palm swamp. Data were collected in  
15    both wet and dry seasons over the course of four field campaigns from 2012 to 2014.  
16    Peatlands in the PMFB were large and regionally significant sources of atmospheric  $\text{CH}_4$ ,  
17    emitting  $36.05 \pm 3.09 \text{ mg CH}_4\text{-C m}^{-2} \text{ d}^{-1}$ .  $\text{CH}_4$  emissions varied significantly among vegetation  
18    types and between seasons.  $\text{CH}_4$  fluxes were greatest for mixed palm swamp ( $52.0 \pm 16.0 \text{ mg}$   
19     $\text{CH}_4\text{-C m}^{-2} \text{ d}^{-1}$ ), followed by *M. flexuosa* palm swamp ( $36.7 \pm 3.9 \text{ mg CH}_4\text{-C m}^{-2} \text{ d}^{-1}$ ), forested  
20    (short pole) vegetation ( $31.6 \pm 6.6 \text{ mg CH}_4\text{-C m}^{-2} \text{ d}^{-1}$ ), and forested vegetation ( $29.8 \pm 10.0 \text{ mg}$   
21     $\text{CH}_4\text{-C m}^{-2} \text{ d}^{-1}$ ).  $\text{CH}_4$  fluxes also showed marked seasonality, with divergent seasonal flux  
22    patterns among ecosystems. Forested vegetation and mixed palm swamp showed  
23    significantly higher dry season ( $47.2 \pm 5.4 \text{ mg CH}_4\text{-C m}^{-2} \text{ d}^{-1}$  and  $85.5 \pm 26.4 \text{ mg CH}_4\text{-C m}^{-2} \text{ d}^{-1}$ ,  
24    respectively) compared to wet season emissions ( $6.8 \pm 1.0 \text{ mg CH}_4\text{-C m}^{-2} \text{ d}^{-1}$  and  $5.2 \pm 2.7 \text{ mg}$   
25     $\text{CH}_4\text{-C m}^{-2} \text{ d}^{-1}$ , respectively). In contrast, forested (short pole) vegetation and *M. flexuosa* palm  
26    swamp showed the opposite trend, with dry season fluxes of  $9.6 \pm 2.6$  and  $25.5 \pm 2.9 \text{ mg CH}_4\text{-C m}^{-2}$   
27     $\text{C m}^{-2} \text{ d}^{-1}$ , respectively, versus wet season fluxes of  $103.4 \pm 13.6$  and  $53.4 \pm 9.8 \text{ mg CH}_4\text{-C m}^{-2}$   
28     $\text{d}^{-1}$ , respectively. Nitrous oxide fluxes were negligible ( $0.70 \pm 0.34 \text{ } \mu\text{g N}_2\text{O-N m}^{-2} \text{ d}^{-1}$ ), and did  
29    not vary significantly among ecosystems or between seasons.

30

31



32 **KEYWORDS**

33 methane, nitrous oxide, peat, tropical peatland, Amazonia, Peru

34

35

36 **3. INTRODUCTION**

37 The Amazon basin plays a critical role in the global atmospheric budgets of carbon (C) and  
38 greenhouse gases (GHGs) such as methane ( $\text{CH}_4$ ) and nitrous oxide ( $\text{N}_2\text{O}$ ). Recent basin-wide  
39 studies suggest that the Amazon as a whole accounts for approximately 7 % of global  
40 atmospheric  $\text{CH}_4$  emissions (Wilson et al., 2016).  $\text{N}_2\text{O}$  emissions are of a similar magnitude,  
41 with emissions ranging from 2-3 Tg  $\text{N}_2\text{O-N year}^{-1}$  (or, approximately 12-18 % of global  
42 atmospheric emissions) (Huang et al., 2008;Saikawa et al., 2014;Saikawa et al., 2013). While  
43 we have a relatively strong understanding of the role that the Amazon plays in regional and  
44 global atmospheric budgets of these gases, one of the key gaps in knowledge is the  
45 contribution of specific ecosystem types to regional fluxes of GHGs (Huang et al.,  
46 2008;Saikawa et al., 2014;Saikawa et al., 2013). In particular, our understanding of the  
47 contribution of Amazonian wetlands to regional C and GHG budgets is weak, as the majority  
48 of past ecosystem-scale studies have focused on *terra firme* forests and savannas (D'Amelio  
49 et al., 2009;Saikawa et al., 2013;Wilson et al., 2016;Kirschke et al., 2013;Nisbet et al., 2014).  
50 Empirical studies of GHG fluxes from Amazonian wetlands are more limited in geographic  
51 scope and have focused on three major areas: wetlands in the state of Amazonas near the  
52 city of Manaus (Devol et al., 1990;Bartlett et al., 1990;Bartlett et al., 1988;Keller et al., 1986),  
53 the Pantanal region (Melack et al., 2004;Marani and Alvalá, 2007;Liengaard et al., 2013), and



54 the Orinoco River basin (Smith et al., 2000;Lavelle et al., 2014). Critically, none of the  
55 ecosystems sampled in the past were peat-forming ones; rather, the habitats investigated  
56 were non-peat forming (i.e. mineral or organo-mineral soils), seasonally-inundated floodplain  
57 forests (i.e. *varzea*), rivers or lakes.

58

59 Peatlands are one of the major wetland habitats absent from current bottom-up GHG  
60 inventories for the Amazon basin, and are often grouped together with non-peat forming  
61 wetlands in regional atmospheric budgets (Wilson et al., 2016). Because we have little or no  
62 data on ecosystem-level land-atmosphere fluxes from these habitats (Lahteenoja et al.,  
63 2012;Lahteenoja et al., 2009b;Kirschke et al., 2013;Nisbet et al., 2014), it is difficult to  
64 ascertain if rates of GHG flux from these ecosystems are similar to or different from mineral  
65 soil wetlands. Given that underlying differences in plant community composition and soil  
66 properties are known to modulate the cycling and flux of GHGs in wetlands (Limpens et al.,  
67 2008;Melton et al., 2013;Belyea and Baird, 2006;Sjögersten et al., 2014), expanding our  
68 observations to include a wider range of wetland habitats is critical in order to improve our  
69 understanding of regional trace gas exchange, and also to determine if aggregating peat and  
70 mineral soil wetlands together in bottom-up emissions inventories are appropriate for  
71 regional budget calculations. Moreover, Amazonian peatlands are thought to account for a  
72 substantial land area (i.e. up to 150,000 km<sup>2</sup>) (Schulman et al., 1999;Lahteenoja et al., 2012),  
73 and any differences in biogeochemistry among peat and mineral/organo-mineral soil  
74 wetlands may therefore have important implications for understanding and modelling the  
75 biogeochemical functioning of the Amazon basin as a whole.

76



77 Since the identification of extensive peat forming wetlands in the north (Lahteenoja et al.,  
78 2009a; Lahateenoja et al. 2009b; Lahteenoja and Page 2011) and south (Householder et al.,  
79 2012) of the Peruvian Amazon, several studies have been undertaken to better characterize  
80 these habitats, investigating vegetation composition and habitat diversity (Draper et al., 2014;  
81 Kelly et al., 2014; Householder et al., 2012; Lahteenoja and Page, 2011), vegetation history  
82 (Lahteenoja and Roucoux et al., 2010), C stocks (Lahteenoja et al., 2012; Draper et al., 2014),  
83 hydrology (Kelly et al., 2014), and peat chemistry (Lahteenoja et al., 2009a; Lahteenoja et al.,  
84 2009b). Most of the studies have focused on the Pastaza-Marañón foreland basin (PMFB),  
85 where one of the largest stretches of contiguous peatlands have been found (Lahteenoja et  
86 al 2009a; Lahteenoja and Page, 2011; Kelly et al, 2014), covering an estimated area of 35,600  
87  $\pm 2,133 \text{ km}^2$  (Draper et al., 2014). Up to 90% of the peatlands in the PMFB lie in flooded  
88 backwater river margins on floodplains and are influenced by large, annual fluctuations in  
89 water table caused by the Amazonian flood pulse (Householder et al., 2012;Lahteenoja et al.,  
90 2009a). These floodplain systems are dominated by shallow ( $\sim 3.9 \text{ m}$ ) (Lahteenoja et al., 2009a)  
91 to deep ( $\sim 12.9 \text{ m}$ ) (Householder et al., 2012) peat deposits. The remaining 10% of these  
92 peatlands are not directly influenced by river flow and form domed (i.e. raised) nutrient-poor  
93 bogs that likely only receive water and nutrients from rainfall (Lahteenoja et al., 2009b). These  
94 nutrient-poor bogs are dominated by large, C-rich forests (termed “pole forests”), that  
95 represent a very high density C store (total pool size of  $1391 \pm 710 \text{ Mg C ha}^{-1}$ , which includes  
96 both above- and belowground stocks); exceeding in fact the C density of nearby floodplain  
97 systems (Draper et al., 2014). Even though the peats in these nutrient-poor bogs have a  
98 relatively high hydraulic conductivity, they act as natural stores of water because of high  
99 rainwater inputs ( $>3000 \text{ mm per annum}$ ), which help to maintain positive water tables, even  
100 during parts of the dry season (Kelly et al., 2014).



101

102 In order to improve our understanding of the biogeochemistry and rates of GHG exchange  
103 from Amazonian peatlands, we conducted a preliminary study of CH<sub>4</sub> and N<sub>2</sub>O fluxes from  
104 forested peatlands in the PMFB. The main objectives of this research were to:

- 105 1. Quantify the magnitude and range of soil CH<sub>4</sub> and N<sub>2</sub>O fluxes from a sub-set of  
106 peatlands in the PMFB that represent key dominant vegetation types
- 107 2. Determine seasonal patterns of trace gas exchange
- 108 3. Establish the relationship between trace gas fluxes and environmental variables

109 Sampling was concentrated on the four most dominant vegetation types in the area, based  
110 on prior work by the investigators (Lahteenoja and Page, 2011). Trace gas fluxes were  
111 captured from both floodplain systems and nutrient-poor bogs in order to account for  
112 underlying differences in biogeochemistry that may arise from variations in hydrology.

113 Sampling was conducted during four field campaigns (two wet season, two dry season) over  
114 a 27-month period, extending from February 2012 to May 2014.

115

116

117 **4. METHODS AND MATERIALS**

118 **4.1 Study site and sampling design**

119 The study was carried out in the lowland tropical peatland forests of the PMFB, between 2  
120 and 35 km south of the city of Iquitos, Peru (Lahteenoja et al., 2009a; Lahteenoja et al., 2009b)  
121 (Figure 1, Table 1). The mean annual temperature is 26 °C, annual precipitation is c. 3,100



122 mm, relative humidity ranges from 80-90 %, and altitude ranges from c. 90 to 130 m above  
123 sea level (Marengo 1998). The northwestern Amazon basin near Iquitos experiences  
124 pronounced seasonality, which is characterized by consistently high annual temperatures, but  
125 marked seasonal variation in precipitation (Tian et al., 1998), and an annual river flood pulse  
126 linked to seasonal discharge from the Andes (Junk et al., 1989). Precipitation events are  
127 frequent, intense and of significant duration during the wet season (November to May) and  
128 infrequent, intense and of short duration during the dry season (June to August). Catchments  
129 in this region receive no less than 100 mm of rain per month (Espinoza Villar et al., 2009a;  
130 Espinoza Villar et al., 2009b) and >3000 mm of rain per year. River discharge varies by season,  
131 with the lowest discharge between the dry season months of August and September. Peak  
132 discharge from the wet season flood pulse occurs between April and May, as recorded at the  
133 Tamshiyaku River gauging station (Espinoza Villar et al., 2009b).

134

135 Soils are classified as pure peat and pure peat with clay and sediment deposits, with an  
136 organic content of >50 %. The pH of the soils varied by site and ranged from 3.5 to 7.2  
137 (Lahteenoja et al., 2009a; Lahteenoja et al., 2009b; this study). Study sites were classified as  
138 either nutrient-rich, intermediate, or nutrient-poor. The former tend to occur on floodplains  
139 and river margins, and account for approximately 90 % of the peatland cover in the PMFB,  
140 and receive water and nutrient inputs from the annual Amazon river flood pulse (Householder  
141 et al., 2012; Lahteenoja et al., 2009a). They are characterized by peat soils which contain  
142 higher inorganic mineral content, of which Ca is a dominant constituent (Lahteenoja et al.,  
143 2009b). In contrast, the nutrient-poor sites tend to occur further in-land (i.e. away from river  
144 margins and floodplains), and receive low or infrequent inputs of water and nutrients from



145 the annual Amazon river flood pulse, and are almost entirely rain-fed (Lahteenoja et al.,  
146 2009b). These systems account for only about 10 % of peatland cover in the PMFB (Draper et  
147 al., 2014). Soil Ca concentrations are significantly lower in these sites compared to the  
148 nutrient-rich ones, with similar concentrations to that of rainwater (Lahteenoja et al., 2009b).

149

150 We established 229 sampling plots ( $\sim 30 \text{ m}^2$  per plot) within five tropical peatland sites that  
151 captured four of the dominant vegetation types in the region (Draper et al.,  
152 2014;Householder et al., 2012;Kelly et al., 2014;Lahteenoja and Page, 2011), and which  
153 encompassed a range of nutrient availabilities (Figure 1, Table 1) (Lahteenoja and Page,  
154 2011;Lahteenoja et al., 2009a). These four dominant vegetation types included: forested  
155 vegetation (nutrient-rich; n= 9 plots), forested (short pole) vegetation (nutrient-poor; n= 19  
156 plots), *Mauritia flexuosa*-dominated palm swamp (intermediate fertility, n= 112 plots), and  
157 mixed palm swamp (nutrient-rich; n=8 plots) (Table 1). Four of the study sites (Buena Vista,  
158 Charo, Miraflores, and Quistococha) were dominated by single vegetation types, whereas San  
159 Jorge contained a mixture of *M. flexuosa* palm swamp and forested (short pole) vegetation  
160 (Table 1). As a consequence, both vegetation types were sampled in San Jorge to develop a  
161 more representative picture of GHG fluxes from this location. Sampling efforts were partially  
162 constrained by issues of site access; some locations were difficult to access (e.g. centre of the  
163 San Jorge peatland) due to water table height and navigability of river channels; as a  
164 consequence, sampling patterns were somewhat uneven, with higher sampling densities in  
165 some peatlands than in others (Table 1).

166



167 In each peatland site, transects were established from the edge of the peatland to its centre.  
168 Each transect varied in length from 2 to 5 km, depending on the relative size of the peatland.  
169 Randomly located sampling plots ( $\sim 30 \text{ m}^2$  per plot) were established at 50 or 200 m intervals  
170 along each transect, from which GHG fluxes and environmental variables were measured  
171 concomitantly. The sampling interval (i.e. 50 or 200 m) was determined by the length of the  
172 transect or size of the peatland, with shorter sampling intervals (50 m) for shorter transects  
173 (i.e. smaller peatlands) and longer sampling intervals (200 m) for longer transects (i.e. larger  
174 peatlands).

175

#### 176 **4.2 Quantifying soil-atmosphere exchange**

177 Soil-atmosphere fluxes ( $\text{CH}_4$ ,  $\text{N}_2\text{O}$ ) were determined in four campaigns over a two-year annual  
178 water cycle: February 2012 (wet season), June-August 2012 (dry season), June-July 2013 (dry  
179 season), and May-June 2014 (wet season). Gas exchange was quantified using a floating static  
180 chamber approach (Livingston and Hutchinson, 1995; Teh et al., 2011). Static flux  
181 measurements were made by enclosing a  $0.225 \text{ m}^2$  area with a dark, single component,  
182 vented 10 L flux chamber. No chamber bases (collars) were used due to the highly saturated  
183 nature of the soils. In most cases, a standing water table was present at the soil surface, so  
184 chambers were placed directly onto the water. In the absence of a standing water table, a  
185 weighted skirt was applied to create an airtight seal. Under these drier conditions, chambers  
186 were placed carefully on the soil surface from a distance of no closer than 2 m in order to  
187 reduce the risk of pressure-induced ebullition or disruption to soil gas concentration profiles  
188 caused by the investigators' footfall. To promote even mixing within the headspace, chambers  
189 were fitted with small computer fans (Pumpanen et al., 2004). Headspace samples were



190 collected from each flux chamber at five intervals over a 25 minute enclosure period using a  
191 gas tight syringe. Gas samples were stored in evacuated Exetainers® (Labco Ltd., Lampeter  
192 UK), shipped to the UK, and subsequently analysed for CH<sub>4</sub>, CO<sub>2</sub> and N<sub>2</sub>O concentrations using  
193 Thermo TRACE GC Ultra (Thermo Fischer Scientific Inc., Waltham, Massachusetts, USA) at the  
194 University of St. Andrews. Chromatographic separation was achieved using a Porapak-Q  
195 column, and gas concentrations determined using a flame ionization detector (FID) for CH<sub>4</sub>, a  
196 methanizer-FID for CO<sub>2</sub>, and an electron capture detector (ECD) for N<sub>2</sub>O. Instrumental  
197 precision, determined from repeated analysis of standards, was < 5% for all detectors. Flux  
198 rates were determined by using the JMP IN version 11 (SAS Institute, Inc., Cary, North  
199 Carolina, USA) package to plot best-fit lines to the data for headspace concentration against  
200 time for individual flux chambers (Teh et al., 2014). Gas mixing ratios (ppm) were converted  
201 to areal fluxes by using the Ideal Gas Law to solve for the quantity of gas in the headspace (on  
202 a mole or mass basis) and normalized by the surface area of each static flux chamber  
203 (Livingston and Hutchinson, 1995).

204

#### 205 **4.3 Environmental variables**

206 To investigate the effects of environmental variables on trace gas fluxes, we determined air  
207 temperature, soil temperature, chamber headspace temperature, soil pH, soil electrical  
208 conductivity (EC;  $\mu\text{Scm}^{-2}$ ), dissolved oxygen concentration of the soil pore water (DO;  
209 measured as percent saturation, %) in the top 15 cm of the peat column, and water table  
210 position concomitant with gas sampling. Air temperature and chamber headspace  
211 temperature were measured using a Check Temp probe and meter. Peat temperature, pH,  
212 DO and EC were measured at a depth of 15 cm below the peat surface and recorded *in situ*



213 with each gas sample using a HACH® rugged outdoor HQ30D multi meter and pH, LDO or EC  
214 probe. At sites where the water level was above the peat surface, the water depth was  
215 measured using a meter rule. Where the water table was at or below the peat surface, the  
216 water level was measured by auguring a hole to 1 m depth and measuring water table depth  
217 using a meter rule.

218

#### 219 **4.4 Statistical Analyses**

220 Statistical analyses were performed using JMP IN version 11 (SAS Institute, Inc., Cary, North  
221 Carolina, USA). Box-Cox transformations were applied where the data failed to meet the  
222 assumptions of analysis of variance (ANOVA); otherwise, non-parametric tests were applied.  
223 ANOVA and analysis of co-variance (ANCOVA) were used to test for relationships between gas  
224 fluxes and vegetation type, season, and environmental variables. When determining the  
225 effect of vegetation type on gas flux, data from different study sites (e.g. San Jorge and  
226 Miraflores) were pooled together. Means comparisons were tested using a Fisher's Least  
227 Significant Difference (LSD) test.

228

229

#### 230 **5. RESULTS**

##### 231 **5. 1 Differences in gas fluxes and environmental variables among vegetation types**

232 All vegetation types were net sources of CH<sub>4</sub>, with an overall mean (± standard error) flux of  
233  $36.1 \pm 3.1 \text{ mg CH}_4\text{-C m}^{-2} \text{ d}^{-1}$ . Soil CH<sub>4</sub> fluxes varied significantly among the four vegetation



234 types sampled in this study (two-way ANOVA with vegetation, season and their interaction,  
235  $F_{7, 979} = 13.2$ ,  $P < 0.0001$ ; Fig. 2a). However, the effect of vegetation was relatively weak (see  
236 ANCOVA results in the section 'Relationships between gas fluxes and environmental  
237 variables'), and a means comparison test on the pooled data was unable to determine which  
238 means differed significantly from the others (Fisher's LSD,  $P > 0.05$ ). For the pooled data, the  
239 overall numerical trend was that mixed palm swamp showed the highest mean flux ( $52.0 \pm$   
240  $16.0 \text{ mg CH}_4\text{-C m}^{-2} \text{ d}^{-1}$ ), followed by *M. flexuosa* palm swamp ( $36.7 \pm 3.9 \text{ mg CH}_4\text{-C m}^{-2} \text{ d}^{-1}$ ),  
241 forested (short pole) vegetation ( $31.6 \pm 6.6 \text{ mg CH}_4\text{-C m}^{-2} \text{ d}^{-1}$ ), and forested vegetation ( $29.8$   
242  $\pm 10.0 \text{ mg CH}_4\text{-C m}^{-2} \text{ d}^{-1}$ ).

243

244 These study sites were also a weak net source of  $\text{N}_2\text{O}$ , with a mean flux of  $0.70 \pm 0.34 \text{ } \mu\text{g N}_2\text{O-}$   
245  $\text{N m}^{-2} \text{ d}^{-1}$ . Because of the high variance in  $\text{N}_2\text{O}$  flux among plots, analysis of variance indicated  
246 that mean  $\text{N}_2\text{O}$  flux did not differ significantly among vegetation types (two-way ANOVA,  $P >$   
247 0.5, Fig. 2b). However, when the  $\text{N}_2\text{O}$  flux data were grouped by vegetation type, we see that  
248 some vegetation types tended to function as net atmospheric sources, while others acted as  
249 atmospheric sinks (Fig. 2b, Table 3). For example, the highest  $\text{N}_2\text{O}$  emissions were observed  
250 from *M. flexuosa* palm swamp ( $1.11 \pm 0.44 \text{ } \mu\text{g N}_2\text{O-N m}^{-2} \text{ d}^{-1}$ ) and forested vegetation ( $0.20 \pm$   
251  $0.95 \text{ } \mu\text{g N}_2\text{O-N m}^{-2} \text{ d}^{-1}$ ). In contrast, forested (short pole) vegetation and mixed palm swamp  
252 were weak sinks for  $\text{N}_2\text{O}$ , with mean fluxes of  $-0.01 \pm 0.84$  and  $-0.21 \pm 0.70 \text{ } \mu\text{g N}_2\text{O-N m}^{-2} \text{ d}^{-1}$ ,  
253 respectively.

254



255 Soil pH varied significantly among vegetation types (data pooled across all seasons; ANOVA,  
256  $P < 0.0001$ , Table 2). Multiple comparisons tests indicated that mean soil pH was significantly  
257 different for each of the vegetation types (Fisher's LSD,  $P < 0.0001$ , Table 2), with the lowest  
258 pH in forested (short pole) vegetation ( $4.10 \pm 0.04$ ), followed by *M. flexuosa* palm swamp  
259 ( $5.32 \pm 0.02$ ), forested vegetation ( $6.15 \pm 0.06$ ), and the mixed palm swamp ( $6.58 \pm 0.04$ ).

260

261 Soil dissolved oxygen (DO) content varied significantly among vegetation types (data pooled  
262 across all seasons; Kruskal-Wallis,  $P < 0.0001$ , Table 2). Multiple comparisons tests indicated  
263 that mean DO was significantly different for each of the vegetation types (Fisher's LSD,  $P <$   
264  $0.05$ , Table 2), with the highest DO in the forested (short pole) vegetation ( $25.2 \pm 2.1 \%$ ),  
265 followed by the *M. flexuosa* palm swamp ( $18.1 \pm 1.0 \%$ ), forested vegetation ( $11.8 \pm 2.8 \%$ ),  
266 and the mixed palm swamp ( $0.0 \pm 0.0 \%$ ).

267

268 Electrical conductivity (EC) varied significantly among vegetation types (data pooled across all  
269 seasons; Kruskal-Wallis,  $P < 0.0001$ , Table 2). Multiple comparison tests indicated that mean  
270 EC was significantly for each of the vegetation types (Fisher's LSD,  $P < 0.05$ ; Table 2), with the  
271 highest EC in the mixed palm swamp ( $170.9 \pm 6.0 \mu\text{s m}^{-2}$ ), followed by forested vegetation  
272 ( $77.1 \pm 4.2 \mu\text{s m}^{-2}$ ), *M. flexuosa* palm swamp ( $49.7 \pm 1.4 \mu\text{s m}^{-2}$ ) and the forested (short pole)  
273 vegetation ( $40.9 \pm 3.5 \mu\text{s m}^{-2}$ ).

274

275 Soil temperature varied significantly among vegetation types (data pooled across all seasons;  
276 ANOVA,  $P < 0.0001$ , Table 2). Multiple comparisons tests indicated that soil temperature in



277 forested (short pole) vegetation was significantly lower than in the other vegetation types  
278 (Table 2); whereas the other vegetation types did not differ in temperature amongst  
279 themselves (Fisher's LSD,  $P < 0.05$ , Table 2).

280

281 Air temperature varied significantly among vegetation types (data pooled across all seasons;  
282 ANOVA,  $P < 0.0001$ , Table 2). Multiple comparisons tests indicated that soil temperature in  
283 *M. flexuosa* palm swamp was significantly lower than in the other vegetation types; whereas  
284 the other vegetation types did not differ in temperature amongst themselves (Fisher's LSD,  $P$   
285  $< 0.05$ , Table 2).

286

287 Water table depths varied significantly among vegetation types (data pooled across all  
288 seasons; ANOVA,  $P < 0.0001$ , Table 2). The highest mean water tables were observed in mixed  
289 palm swamp ( $59.6 \pm 9.3$  cm), followed by forested vegetation ( $34.0 \pm 6.9$  cm), *M. flexuosa*  
290 palm swamp ( $17.4 \pm 1.2$  cm), and forested (short pole) vegetation ( $3.5 \pm 1.0$  cm) (Fisher's LSD,  
291  $P < 0.0005$ ).

292

## 293 **5.2 Seasonal variations in gas fluxes and environmental variables**

294 The peatlands sampled in this study showed pronounced seasonal variability in  $\text{CH}_4$  fluxes  
295 (two-way ANOVA,  $F_{7, 979} = 13.2$ ,  $P < 0.0001$ ; Table 3). In contrast,  $\text{N}_2\text{O}$  fluxes showed no  
296 seasonal trends (two-way ANOVA,  $P > 0.5$ ), and therefore will not be discussed further here.  
297 For  $\text{CH}_4$  flux, the overall trend was towards significantly higher wet season ( $51.1 \pm 7.0$  mg  $\text{CH}_4$ -



298  $\text{C m}^{-2} \text{d}^{-1}$ ) compared to dry season ( $27.3 \pm 2.7 \text{ mg CH}_4\text{-C m}^{-2} \text{d}^{-1}$ ) fluxes (data pooled across all  
299 vegetation types; t-Test,  $P < 0.001$ , Table 3). However, when the  $\text{CH}_4$  fluxes were  
300 disaggregated by vegetation type, very different seasonal trends emerged. For example, both  
301 forested vegetation and mixed palm swamp showed significantly greater  $\text{CH}_4$  fluxes during  
302 the *dry season* with net fluxes of  $47.2 \pm 5.4 \text{ mg CH}_4\text{-C m}^{-2} \text{d}^{-1}$  and  $64.2 \pm 12.1 \text{ mg CH}_4\text{-C m}^{-2}$   
303  $\text{d}^{-1}$ , respectively (Fisher's LSD,  $P < 0.05$ , Table 3). In contrast, *wet season* fluxes were 7-16  
304 times lower, with net fluxes of  $6.7 \pm 1.0 \text{ mg CH}_4\text{-C m}^{-2} \text{d}^{-1}$  and  $6.1 \pm 1.3 \text{ mg CH}_4\text{-C m}^{-2} \text{d}^{-1}$ ,  
305 respectively (Fisher's LSD,  $P < 0.05$ , Table 3). In contrast, forested (short pole) vegetation and  
306 *M. flexuosa* palm swamp showed seasonal trends consistent with the pooled data set; i.e.  
307 significantly higher fluxes during the wet season ( $46.7 \pm 8.4$  and  $60.4 \pm 9.1 \text{ mg CH}_4\text{-C m}^{-2} \text{d}^{-1}$ ,  
308 respectively) compared to the dry season ( $28.3 \pm 2.6$  and  $18.8 \pm 2.6 \text{ mg CH}_4\text{-C m}^{-2} \text{d}^{-1}$ ,  
309 respectively) (Fisher's LSD,  $P < 0.05$ , Table 3).

310

311 For the environmental variables, soil pH, DO, EC, water table depth, and soil temperature  
312 varied significantly between seasons, whereas air temperature did not. Thus, for sake of  
313 brevity, air temperature is not discussed further here. Mean soil pH was significantly lower  
314 during the wet season ( $5.18 \pm 0.03$ ) than the dry season ( $5.31 \pm 0.04$ ) (data pooled across all  
315 vegetation types; t-Test,  $P < 0.05$ , Table 2). When disaggregated by vegetation type, the  
316 overall trend was found to hold true for all vegetation types except forested (short pole)  
317 vegetation, which displayed higher pH during the wet season compared to the dry season  
318 (Table 2). A two-way ANOVA on Box-Cox transformed data using vegetation type, season and  
319 their interaction as explanatory variables indicated that vegetation type was the best



320 predictor of pH, with season and vegetation type by season playing a lesser role ( $F_{7, 1166} =$   
321 348.9,  $P < 0.0001$ ).

322

323 For DO, the overall trend was towards significantly lower DO during the wet season ( $13.9 \pm$   
324 1.0 %) compared to the dry season ( $19.3 \pm 1.2$  %) (data pooled across all vegetation types;  
325 Wilcoxon test,  $P < 0.0001$ , Table 2). However, when the data were disaggregated by  
326 vegetation type, we found that individual vegetation types showed distinct seasonal trends  
327 from each other. Forested vegetation and mixed palm swamp were consistent with the  
328 overall trend (i.e. lower wet season compared to dry season DO), whereas forested (short  
329 pole) vegetation and *M. flexuosa* palm swamp displayed the reverse trend (i.e. higher wet  
330 season compared to dry season DO) (Table 2). A two-way ANOVA on Box Cox transformed  
331 data using vegetation type, season and their interaction as explanatory variables indicated  
332 that vegetation type was the best predictor of DO, followed by a strong vegetation by season  
333 interaction; season itself played a lesser role than either of the other two explanatory  
334 variables ( $F_{7, 1166} = 57.0$ ,  $P < 0.0001$ ).

335

336 For EC, the overall trend was towards lower EC in the wet season ( $49.4 \pm 1.8 \mu\text{s m}^{-2}$ ) compared  
337 to the dry season ( $65.5 \pm 2.2 \mu\text{s m}^{-2}$ ) (data pooled across all vegetation types; Wilcoxon test,  
338  $P < 0.05$ , Table 2). When the data were disaggregated by vegetation type, this trend was  
339 consistent for all the vegetation types except for forested vegetation, where differences  
340 between wet and dry season were not statistically significant (Wilcoxon,  $P > 0.05$ , Table 2).

341



342 Water table depths varied significantly between seasons (data pooled across all vegetation  
343 types; Wilcoxon test,  $P < 0.0001$ , Table 2). Mean water table level was significantly higher in  
344 the wet ( $54.1 \pm 2.7$  cm) than the dry ( $1.3 \pm 0.8$  cm) season. When disaggregated by vegetation  
345 type, the trend held true for individual vegetation types (Table 2). All vegetation types had  
346 negative dry season water tables (i.e. below the soil surface) and positive wet season water  
347 tables (i.e. water table above the soil surface), except for *M. flexuosa* palm swamp that had  
348 positive water tables in both seasons. Two-way ANOVA on Box-Cox transformed data using  
349 vegetation type, season and their interaction as explanatory variables indicated that all three  
350 factors explained water table depth, but that season accounted for the largest proportion of  
351 the variance in the model, followed by vegetation by season, and lastly by vegetation type ( $F_{7, 1157} = 440.1$ ,  $P < 0.0001$ ).

353

354 For soil temperature, the overall trend was towards slightly higher temperatures in the wet  
355 season ( $25.6 \pm 0.0^\circ\text{C}$ ) compared to the dry season ( $25.1 \pm 0.0^\circ\text{C}$ ) (t-Test,  $P < 0.0001$ ). Analysis  
356 of the disaggregated data indicates this trend was consistent for individual vegetation types  
357 (Table 2). Two-way ANOVA on Box-Cox transformed data using vegetation type, season and  
358 their interaction as explanatory variables indicated that all three variables played a significant  
359 role in modulating soil temperature, although season accounted for the largest proportion of  
360 the variance whereas the other two factors accounted for a similar proportion of the variance  
361 ( $F_{7, 1166} = 21.3$ ,  $P < 0.0001$ ).

362

363 **5.3 Relationships between gas fluxes and environmental variables**



364 To explore the relationship between environmental variables and trace gas fluxes, we  
365 conducted an analysis of covariance (ANCOVA) on Box-Cox transformed gas flux data, using  
366 vegetation type, season, vegetation by season, and environmental variables as explanatory  
367 variables.

368

369 For CH<sub>4</sub>, ANCOVA revealed that vegetation by season was the strongest predictor of CH<sub>4</sub> flux,  
370 followed by a strong season effect ( $F_{13, 917} = 9.2, P < 0.0001$ ). Other significant drivers included  
371 soil temperature, water table depth, and a borderline-significant effect of vegetation type ( $P$   
372  $< 0.06$ ). The strong effect of vegetation by season reflects the fact that different vegetation  
373 types showed seasonal differences in emission patterns, with forested vegetation and mixed  
374 palm swamp showing significantly higher dry season compared to wet season emissions,  
375 while forested (short pole) vegetation and *M. flexuosa* palm swamp showed the reverse trend  
376 (see above; Table 3). The positive relationships between soil temperature, water table depth  
377 and CH<sub>4</sub> flux indicate that warmer conditions or higher water tables both stimulate CH<sub>4</sub> flux.  
378 However, it is important to note that each of these environmental variables were only weakly  
379 correlated with CH<sub>4</sub> flux even if the relationships were statistically significant; when individual  
380 bivariate regressions were calculated, the  $r^2$  values were less than 0.01 for each plot.

381

382 For N<sub>2</sub>O, ANCOVA indicated that the best predictors of flux rates were dissolved oxygen and  
383 conductivity ( $F_{13, 1014} = 2.2, P < 0.0082$ ). As was the case for CH<sub>4</sub> and CO<sub>2</sub>, when the  
384 relationships between these environmental variables and N<sub>2</sub>O flux were explored using



385 individual bivariate regressions,  $r^2$  values were found to be very low (e.g. less than  $r^2 < 0.0009$ )  
386 and not statistically significant.

387

388

389 **6. DISCUSSION**

390 **6.1 Large and asynchronous CH<sub>4</sub> fluxes from peatlands in the Pastaza-Marañón foreland**  
391 **basin**

392 The ecosystems sampled in this study were strong atmospheric sources of CH<sub>4</sub>. Net CH<sub>4</sub> flux,  
393 averaged across all vegetation types, was  $36.1 \pm 3.1$  mg CH<sub>4</sub>-C m<sup>-2</sup> d<sup>-1</sup>, spanning a range from  
394 -99.8 to 1,509.7 mg CH<sub>4</sub>-C m<sup>-2</sup> d<sup>-1</sup>. This mean falls within the range of fluxes observed in  
395 Indonesian peatlands (3.7-87.8 mg CH<sub>4</sub>-C m<sup>-2</sup> d<sup>-1</sup>) (Couwenberg et al., 2010) and other  
396 Amazonian wetlands (7.1-390.0 mg CH<sub>4</sub>-C m<sup>-2</sup> d<sup>-1</sup>) (Bartlett et al., 1990;Bartlett et al.,  
397 1988;Devol et al., 1990;Devol et al., 1988). These data suggest that peatlands in the Pastaza-  
398 Marañón foreland basin may be strong contributors to the regional atmospheric CH<sub>4</sub> budget,  
399 given that the four vegetation types sampled here represent the dominant cover types in the  
400 PMFB (Draper et al., 2014;Householder et al., 2012;Kelly et al., 2014;Lahteenoja and Page,  
401 2011)

402

403 The overall trend in the data was towards greater temporal (i.e. seasonal) variability in CH<sub>4</sub>  
404 fluxes rather than spatial (i.e. inter-site) variability. For the pooled dataset, CH<sub>4</sub> emissions  
405 were significantly greater during the wet season than the dry season, with fluxes falling by



406 approximately half from one season to the other (i.e.  $51.1 \pm 7.0$  to  $27.3 \pm 2.7$  mg CH<sub>4</sub>-C m<sup>-2</sup>  
407 d<sup>-1</sup>). This is in contrast to the data on CH<sub>4</sub> fluxes among study sites, where statistical analyses  
408 indicate that there was a weak effect of vegetation type on CH<sub>4</sub> flux, that was on the edge of  
409 statistical significance (i.e. ANCOVA;  $P < 0.06$  for the vegetation effect term).

410

411 On face value, these data suggest two findings; first, the weak effect of vegetation type  
412 implies that patterns of CH<sub>4</sub> cycling are broadly similar among study sites. Second, the strong  
413 seasonal pattern suggests that – on the whole – these systems conform to our normative  
414 expectations of how peatlands function with respect to seasonal variations in hydrology and  
415 redox potential; i.e. enhanced CH<sub>4</sub> emissions during a more anoxic wet season, and reduced  
416 CH<sub>4</sub> emissions during a more oxic dry season when water tables fall. However, closer  
417 inspection of the data reveals that different vegetation types showed contrasting seasonal  
418 emission patterns (Table 3), challenging our basic assumptions about how these ecosystems  
419 function. For example, while forested (short pole) vegetation and *M. flexuosa* palm swamp  
420 conformed to expected seasonal trends for methanogenic wetlands (i.e. higher wet season  
421 compared to dry season emissions), forested vegetation and mixed palm swamp showed the  
422 opposite pattern, with significantly greater CH<sub>4</sub> emissions during the dry season. The  
423 disaggregated data thus imply that the process-based controls on CH<sub>4</sub> fluxes may vary  
424 significantly among these different ecosystems, rather than being similar, leading to a  
425 divergence in seasonal flux patterns.

426



427 What may explain this pattern of divergence? One explanation is that CH<sub>4</sub> emissions from  
428 forested vegetation and mixed palm swamp, compared to the other two ecosystems, may be  
429 more strongly transport-limited during the wet season than the dry season. This  
430 interpretation is partially supported by the field data; forested vegetation and mixed palm  
431 swamp had the highest wet season water table levels, measuring 110.8 ± 9.3 and 183.7 ± 1.7  
432 cm, respectively (Table 2). In contrast, water table levels for forested (short pole) vegetation  
433 and *M. flexuosa* palm swamp in the wet season were 3–7 times lower, measuring only 26.9 ±  
434 0.5 and 37.2 ± 1.7 cm, respectively (Table 2). The greater depth of overlying water in forested  
435 vegetation and mixed palm swamp may therefore have exerted a greater physical constraint  
436 on gas transport compared to the other two ecosystems. Although one could argue that the  
437 positive relationship between water table depth and CH<sub>4</sub> flux found in the ANCOVA  
438 contradicts this interpretation, the relationship between the two variables is so weak (i.e.  $r^2$   
439 = 0.005) that we believe it is unlikely that water table alone exerted a strong control over CH<sub>4</sub>  
440 fluxes.

441

442 However, transport limitation alone does not fully explain the difference in dry season CH<sub>4</sub>  
443 emissions among vegetation types. Forested vegetation and mixed palm swamp showed  
444 substantially higher dry season CH<sub>4</sub> emissions (47.2 ± 5.4 and 85.5 ± 26.4 mg CH<sub>4</sub>-C m<sup>-2</sup> d<sup>-1</sup>,  
445 respectively) compared to forested (short pole) vegetation and *M. flexuosa* palm swamp (9.6  
446 ± 2.6 and 25.5 ± 2.9 mg CH<sub>4</sub>-C m<sup>-2</sup> d<sup>-1</sup>, respectively), pointing to underlying differences in CH<sub>4</sub>  
447 production and oxidation among these ecosystems. One possibility is that dry season  
448 methanogenesis in forested vegetation and mixed palm swamp was greater than in the other  
449 two ecosystems, potentially driven by higher rates of C flow (Whiting and Chanton, 1993).



450 This is plausible given that forested vegetation and mixed palm swamp tend to occur in more  
451 nutrient-rich parts of the Pastaza-Marañón foreland basin, whereas forested (short pole)  
452 vegetation and *M. flexuosa* palm swamp tend to dominate in more nutrient-poor areas  
453 (Lahteenoja et al., 2009a), leading to potential differences in rates of plant productivity.  
454 Moreover, it is possible that the nutrient-rich vegetation may be able to utilize the higher  
455 concentration of nutrients, deposited during the flood pulse, during the Amazonian dry  
456 season (Morton et al., 2014; Saleska et al., 2016), with implications for overall ecosystem C  
457 throughput and CH<sub>4</sub> emissions. Of course, this interpretation does not preclude other  
458 explanations, such as differences in CH<sub>4</sub> transport rates among ecosystems (e.g. due to plant-  
459 facilitated transport or ebullition) (Panagala et al., 2013), or varying rates of CH<sub>4</sub> oxidation  
460 (Teh et al., 2005); however, these possibilities cannot be explored further without recourse  
461 to more detailed process-level experiments. Forthcoming studies on the regulation of GHG  
462 fluxes at finer spatial scales (e.g. investigation of environmental gradients within individual  
463 study sites) or diurnal patterns of GHG exchange (Murphy et al., in prep.) will further deepen  
464 our understanding of the process controls on soil GHG flux from these peatlands, and shed  
465 light on these questions.

466

467 Finally, while the trends described here are intriguing, it is important to acknowledge some  
468 of the potential limitations of our data. First, given the uneven sampling pattern, it is possible  
469 that the values reported here do not fully represent the entire range of fluxes for the more  
470 lightly sampled habitats. However, given the large and statistically significant differences in  
471 CH<sub>4</sub> fluxes during different seasons, it is likely that the main trends that we have identified  
472 here will hold true with more spatially-extensive sampling. Second, the data presented here



473 represent a conservative estimate of CH<sub>4</sub> efflux because the low frequency sampling approach  
474 utilized in this study was unable to capture “hot moments” or erratic ebullition fluxes, which  
475 often result in much higher net CH<sub>4</sub> fluxes (McClain et al., 2003). Third and last, our data  
476 probably underestimate net CH<sub>4</sub> fluxes for the PMFB because we chose to include fluxes with  
477 strong negative values (i.e. more than -10 mg CH<sub>4</sub>-C m<sup>-2</sup> d<sup>-1</sup>) in our calculation of mean flux  
478 rates. These observations are more negative than other values typically reported elsewhere  
479 in the tropical wetland literature (Bartlett et al., 1990;Bartlett et al., 1988;Devol et al.,  
480 1990;Devol et al., 1988;Couwenberg et al., 2010). However, they represent only a small  
481 proportion of our dataset (i.e. 7 %, or only 68 out of 980 measurements), and inspection of  
482 our field notes and the data itself did not produce convincing reasons to exclude these  
483 observations (e.g. we found no evidence of irregularities during field sampling, and any  
484 chambers that showed statistically insignificant changes in concentration over time were  
485 removed during our quality control procedures). While headspace concentrations for these  
486 measurements were often elevated above mean tropospheric levels (>2 ppm), this in itself is  
487 not unusual in reducing environments that contain strong local sources of CH<sub>4</sub> (Baldocchi et  
488 al., 2012). We did not see this as a reason to omit these values as local concentrations of CH<sub>4</sub>  
489 are likely to vary naturally in methanogenic forest environments because of poor mixing in  
490 the understory. Most importantly, exclusion of these data did not alter the overall statistical  
491 trends reported above, and only produced slightly higher estimates of mean CH<sub>4</sub> flux (41.6 ±  
492 3.2 mg CH<sub>4</sub>-C m<sup>-2</sup> d<sup>-1</sup> versus 36.1 ± 3.1 mg CH<sub>4</sub>-C m<sup>-2</sup> d<sup>-1</sup>).

493

494 **6.2 Western Amazonian peatlands as weak atmospheric sources of nitrous oxide**



495 The ecosystems sampled in this study were negligible atmospheric sources of  $\text{N}_2\text{O}$ , emitting  
496 only  $0.70 \pm 0.34 \mu\text{g N}_2\text{O-N m}^{-2} \text{d}^{-1}$ , suggesting that peatlands in the Pastaza-Marañón foreland  
497 basin make little or no contribution to regional atmospheric budgets of  $\text{N}_2\text{O}$ . This is consistent  
498 with  $\text{N}_2\text{O}$  flux measurements from other forested tropical peatlands, where  $\text{N}_2\text{O}$  emissions  
499 were also found to be relatively low (Inubushi et al., 2003; Couwenberg et al., 2010). No  
500 statistically significant differences in  $\text{N}_2\text{O}$  flux were observed among study sites or between  
501 seasons, suggesting that these different peatlands may have similar patterns of  $\text{N}_2\text{O}$  cycling.  
502 Interestingly, differences in  $\text{N}_2\text{O}$  fluxes were not associated with the nutrient status of the  
503 peatland; i.e. more nutrient-rich ecosystems, such as forested vegetation and mixed palm  
504 swamp, did not show higher  $\text{N}_2\text{O}$  fluxes than their nutrient-poor counterparts, such as  
505 forested (short pole) vegetation and *M. flexuosa* palm swamp. This may imply that N  
506 availability, one of the principal drivers of nitrification, denitrification, and  $\text{N}_2\text{O}$  production  
507 (Groffman et al., 2009; Werner et al., 2007), may not be greater in nutrient-rich versus  
508 nutrient-poor ecosystems in this part of the Western Amazon. Alternatively, it is possible that  
509 even though N availability and N fluxes may differ between nutrient-rich and nutrient-poor  
510 systems,  $\text{N}_2\text{O}$  yield may also vary such that net  $\text{N}_2\text{O}$  emissions are not significantly different  
511 among study sites (Teh et al., 2014).

512

513 One potential source of concern are the negative  $\text{N}_2\text{O}$  fluxes that we documented here. While  
514 some investigators have attributed negative fluxes to instrumental error (Cowan et al.,  
515 2014; Chapuis-Lardy et al., 2007), others have demonstrated that  $\text{N}_2\text{O}$  consumption –  
516 particularly in wetland soils – is not an experimental artifact, but occurs due to the complex  
517 effects of redox, organic carbon content, nitrate availability, and soil transport processes on  
518 denitrification (Ye and Horwath, 2016; Yang et al., 2011; Wen et al., 2016; Schlesinger,



519 2013;Teh et al., 2014;Chapuis-Lardy et al., 2007). Given the low redox potential and high  
520 carbon content of these soils, it is plausible that microbial N<sub>2</sub>O consumption is occurring,  
521 because these types of conditions have been found to be conducive for N<sub>2</sub>O uptake elsewhere  
522 (Ye and Horwath, 2016;Teh et al., 2014;Yang et al., 2011).

523

524

525 **7. CONCLUSIONS**

526 These data suggest that peatlands in the Pastaza-Marañón foreland basin are strong sources  
527 of atmospheric CH<sub>4</sub> at a regional scale, and need to be better accounted for in CH<sub>4</sub> emissions  
528 inventories for the Amazon basin as a whole. In contrast, N<sub>2</sub>O fluxes were negligible,  
529 suggesting that these ecosystems are weak regional sources at best. Most intriguing is the  
530 divergent seasonal emissions pattern for CH<sub>4</sub> among different vegetation types, which  
531 challenges our understanding and assumptions of how tropical peatlands function. These  
532 data highlight the need for more spatially-extensive sampling, in order to establish if this  
533 pattern is commonplace across peatlands of the Amazon basin, or if it is unique to the Pastaza-  
534 Marañón foreland basin. If CH<sub>4</sub> emission patterns for different peatlands in the Amazon are  
535 in fact asynchronous and decoupled from rainfall seasonality, then this may partially explain  
536 some of the heterogeneity in CH<sub>4</sub> source and sinks observed at the basin-wide scale (Wilson  
537 et al., 2016).



538 **8. AUTHOR CONTRIBUTION**

539 YAT secured the funding for this research, assisted in the planning and design of the  
540 experiment, and took the principal role in the analysis of the data and preparation of the  
541 manuscript. WAM planned and designed the experiment, collected the field data, analyzed  
542 the samples, and took a secondary role in data preparation, data analysis, and manuscript  
543 preparation. JCB, AB, and SEP supported the planning and design of the experiment, and  
544 provided substantive input into the writing of the manuscript.

545

546

547 **9. ACKNOWLEDGEMENTS**

548 The authors would like to acknowledge the UK Natural Environment Research Council for  
549 funding this research (NERC award number NE/I015469). We would like to thank MINAG and  
550 the Ministerio de Turismo in Iquitos for permits to conduct this research, the Instituto de  
551 Investigaciones de la Amazonía Peruana (IIAP) for logistical support, Peruvian rainforest  
552 villagers for their warm welcome and acceptance, Hugo Vasquez, Pierro Vasquez, Gian Carlo  
553 Padilla Tenazoa and Yully Rojas Reátegui for fieldwork assistance, Dr Outi Lahteenoja and Dr  
554 Ethan Householder for fieldwork planning, and Dr Paul Beaver of Amazonia Expeditions for  
555 lodging and logistical support. Our gratitude also goes to Alex Cumming for fieldwork support  
556 and laboratory assistance, Bill Hickin, Gemma Black, Adam Cox, Charlotte Langley, Kerry Allen,  
557 and Lisa Barber of the University of Leicester for all of their continued support. Thanks are  
558 also owed to Graham Hambley (St Andrews), Angus Calder (St Andrews), Viktoria Oliver  
559 (Aberdeen), Torsten Diem (Aberdeen), Tom Kelly (Leeds), and Freddie Draper (Leeds) for their



560 help in the laboratory and with fieldwork planning. TD, VO, and two anonymous referees  
561 provided very helpful and constructive comments on earlier drafts of this manuscript. This  
562 publication is a contribution from the Scottish Alliance for Geoscience, Environment and  
563 Society (<http://www.sages.ac.uk>) and the UK Tropical Peatland Working Group  
564 (<https://tropicalpeat.wordpress.com>).

565

566

567 **10. REFERENCES**

568 Baldocchi, D., Detto, M., Sonnentag, O., Verfaillie, J., Teh, Y. A., Silver, W., and Kelly, N. M.:  
569 The challenges of measuring methane fluxes and concentrations over a peatland pasture,  
570 Agric. For. Meteorol., 153, 177-187, <http://dx.doi.org/10.1016/j.agrformet.2011.04.013>, 2012.  
571 Bartlett, K. B., Crill, P. M., Sebacher, D. I., Harriss, R. C., Wilson, J. O., and Melack, J. M.:  
572 METHANE FLUX FROM THE CENTRAL AMAZONIAN FLOODPLAIN, Journal of Geophysical  
573 Research-Atmospheres, 93, 1571-1582, 1988.  
574 Bartlett, K. B., Crill, P. M., Bonassi, J. A., Richey, J. E., and Harriss, R. C.: METHANE FLUX  
575 FROM THE AMAZON RIVER FLOODPLAIN - EMISSIONS DURING RISING WATER, Journal of  
576 Geophysical Research-Atmospheres, 95, 16773-16788, 10.1029/JD095iD10p16773, 1990.  
577 Belyea, L. R., and Baird, A. J.: Beyond "The limits to peat bog growth": Cross-scale feedback  
578 in peatland development, Ecological Monographs, 76, 299-322, 2006.  
579 Chapuis-Lardy, L., Wrage, N., Metay, A., Chotte, J.-L., and Bernoux, M.: Soils, a sink for N<sub>2</sub>O?  
580 A review, Global Change Biology, 13, 1-17, 10.1111/j.1365-2486.2006.01280.x, 2007.



581 Couwenberg, J., Dommain, R., and Joosten, H.: Greenhouse gas fluxes from tropical  
582 peatlands in south-east Asia, *Global Change Biology*, 16, 1715-1732, 10.1111/j.1365-  
583 2486.2009.02016.x, 2010.

584 Cowan, N. J., Famulari, D., Levy, P. E., Anderson, M., Reay, D. S., and Skiba, U. M.:  
585 Investigating uptake of N<sub>2</sub>O in agricultural soils using a high-precision dynamic  
586 chamber method, *Atmos. Meas. Tech.*, 7, 4455-4462, 10.5194/amt-7-4455-2014, 2014.

587 D'Amelio, M. T. S., Gatti, L. V., Miller, J. B., and Tans, P.: Regional N<sub>2</sub>O fluxes in Amazonia  
588 derived from aircraft vertical profiles, *Atmospheric Chemistry and Physics*, 9, 8785-8797,  
589 2009.

590 Devol, A. H., Richey, J. E., Clark, W. A., King, S. L., and Martinelli, L. A.: Methane emissions to  
591 the troposphere from the Amazon floodplain, *Journal of Geophysical Research:*  
592 *Atmospheres*, 93, 1583-1592, 10.1029/JD093iD02p01583, 1988.

593 Devol, A. H., Richey, J. E., Forsberg, B. R., and Martinelli, L. A.: SEASONAL DYNAMICS IN  
594 METHANE EMISSIONS FROM THE AMAZON RIVER FLOODPLAIN TO THE TROPOSPHERE,  
595 *Journal of Geophysical Research-Atmospheres*, 95, 16417-16426,  
596 10.1029/JD095iD10p16417, 1990.

597 Draper, F. C., Roucoux, K. H., Lawson, I. T., Mitchard, E. T. A., Coronado, E. N. H., Lahteenoja,  
598 O., Montenegro, L. T., Sandoval, E. V., Zarate, R., and Baker, T. R.: The distribution and  
599 amount of carbon in the largest peatland complex in Amazonia, *Environmental Research*  
600 *Letters*, 9, 12, 10.1088/1748-9326/9/12/124017, 2014.

601 Groffman, P. M., Butterbach-Bahl, K., Fulweiler, R. W., Gold, A. J., Morse, J. L., Stander, E. K.,  
602 Tague, C., Tonitto, C., and Vidon, P.: Challenges to incorporating spatially and temporally  
603 explicit phenomena (hotspots and hot moments) in denitrification models, *Biogeochemistry*,  
604 93, 49-77, 10.1007/s10533-008-9277-5, 2009.



605 Householder, J. E., Janovec, J., Tobler, M., Page, S., and Lähteenoja, O.: Peatlands of the  
606 Madre de Dios River of Peru: Distribution, Geomorphology, and Habitat Diversity, *Wetlands*,  
607 32, 359-368, 10.1007/s13157-012-0271-2, 2012.

608 Huang, J., Golombek, A., Prinn, R., Weiss, R., Fraser, P., Simmonds, P., Dlugokencky, E. J.,  
609 Hall, B., Elkins, J., Steele, P., Langenfelds, R., Krummel, P., Dutton, G., and Porter, L.:  
610 Estimation of regional emissions of nitrous oxide from 1997 to 2005 using multinetwork  
611 measurements, a chemical transport model, and an inverse method, *Journal of Geophysical  
612 Research-Atmospheres*, 113, 1-19, D17313  
613 10.1029/2007jd009381, 2008.

614 Keller, M., Kaplan, W. A., and Wofsy, S. C.: EMISSIONS OF N<sub>2</sub>O, CH<sub>4</sub> AND CO<sub>2</sub> FROM  
615 TROPICAL FOREST SOILS, *Journal of Geophysical Research-Atmospheres*, 91, 1791-1802,  
616 10.1029/JD091iD11p11791, 1986.

617 Kelly, T. J., Baird, A. J., Roucoux, K. H., Baker, T. R., Honorio Coronado, E. N., Ríos, M., and  
618 Lawson, I. T.: The high hydraulic conductivity of three wooded tropical peat swamps in  
619 northeast Peru: measurements and implications for hydrological function, *Hydrological  
620 Processes*, 28, 3373-3387, 10.1002/hyp.9884, 2014.

621 Kirschke, S., Bousquet, P., Ciais, P., Saunois, M., Canadell, J. G., Dlugokencky, E. J.,  
622 Bergamaschi, P., Bergmann, D., Blake, D. R., Bruhwiler, L., Cameron-Smith, P., Castaldi, S.,  
623 Chevallier, F., Feng, L., Fraser, A., Heimann, M., Hodson, E. L., Houweling, S., Josse, B.,  
624 Fraser, P. J., Krummel, P. B., Lamarque, J. F., Langenfelds, R. L., Le Quere, C., Naik, V.,  
625 O'Doherty, S., Palmer, P. I., Pison, I., Plummer, D., Poulter, B., Prinn, R. G., Rigby, M.,  
626 Ringeval, B., Santini, M., Schmidt, M., Shindell, D. T., Simpson, I. J., Spahni, R., Steele, L. P.,  
627 Strode, S. A., Sudo, K., Szopa, S., van der Werf, G. R., Voulgarakis, A., van Weele, M., Weiss,



628 R. F., Williams, J. E., and Zeng, G.: Three decades of global methane sources and sinks,  
629 Nature Geoscience, 6, 813-823, 10.1038/ngeo1955, 2013.

630 Lahteenoja, O., Ruokolainen, K., Schulman, L., and Alvarez, J.: Amazonian floodplains  
631 harbour minerotrophic and ombratrophic peatlands, Catena, 79, 140-145,  
632 10.1016/j.catena.2009.06.006, 2009a.

633 Lahteenoja, O., Ruokolainen, K., Schulman, L., and Oinonen, M.: Amazonian peatlands: an  
634 ignored C sink and potential source, Global Change Biology, 15, 2311-2320, 10.1111/j.1365-  
635 2486.2009.01920.x, 2009b.

636 Lahteenoja, O., and Page, S.: High diversity of tropical peatland ecosystem types in the  
637 Pastaza-Maranon basin, Peruvian Amazonia, Journal of Geophysical Research-  
638 Biogeosciences, 116, 14, 10.1029/2010jg001508, 2011.

639 Lahteenoja, O., Reategui, Y. R., Rasanen, M., Torres, D. D., Oinonen, M., and Page, S.: The  
640 large Amazonian peatland carbon sink in the subsiding Pastaza-Maranon foreland basin,  
641 Peru, Global Change Biology, 18, 164-178, 10.1111/j.1365-2486.2011.02504.x, 2012.

642 Lavelle, P., Rodriguez, N., Arguello, O., Bernal, J., Botero, C., Chaparro, P., Gomez, Y.,  
643 Gutierrez, A., Hurtado, M. D., Loaiza, S., Pullido, S. X., Rodriguez, E., Sanabria, C., Velasquez,  
644 E., and Fonte, S. J.: Soil ecosystem services and land use in the rapidly changing Orinoco  
645 River Basin of Colombia, Agriculture Ecosystems & Environment, 185, 106-117,  
646 10.1016/j.agee.2013.12.020, 2014.

647 Liengaard, L., Nielsen, L. P., Revsbech, N. P., Priem, A., Elberling, B., Enrich-Prast, A., and  
648 Kuhl, M.: Extreme emission of N<sub>2</sub>O from tropical wetland soil (Pantanal, South America),  
649 Frontiers in Microbiology, 3, 13, 10.3389/fmicb.2012.00433, 2013.



650 Limpens, J., Berendse, F., Blodau, C., Canadell, J. G., Freeman, C., Holden, J., Roulet, N.,  
651 Rydin, H., and Schaepman-Strub, G.: Peatlands and the carbon cycle: from local processes to  
652 global implications – a synthesis, *Biogeosciences*, 5, 1475–1491, 2008.  
653 Marani, L., and Alvalá, P. C.: Methane emissions from lakes and floodplains in Pantanal,  
654 Brazil, *Atmospheric Environment*, 41, 1627-1633,  
655 <http://dx.doi.org/10.1016/j.atmosenv.2006.10.046>, 2007.  
656 McClain, M. E., Boyer, E. W., Dent, C. L., Gergel, S. E., Grimm, N. B., Groffman, P. M., Hart, S.  
657 C., Harvey, J. W., Johnston, C. A., Mayorga, E., McDowell, W. H., and Pinay, G.:  
658 Biogeochemical hot spots and hot moments at the interface of terrestrial and aquatic  
659 ecosystems, *Ecosystems*, 6, 301-312, 10.1007/s10021-003-0161-9, 2003.  
660 Melack, J. M., Hess, L. L., Gastil, M., Forsberg, B. R., Hamilton, S. K., Lima, I. B. T., and Novo,  
661 E.: Regionalization of methane emissions in the Amazon Basin with microwave remote  
662 sensing, *Global Change Biology*, 10, 530-544, 10.1111/j.1529-8817.2003.00763.x, 2004.  
663 Melton, J. R., Wania, R., Hodson, E. L., Poulter, B., Ringeval, B., Spahni, R., Bohn, T., Avis, C.  
664 A., Beerling, D. J., Chen, G., Eliseev, A. V., Denisov, S. N., Hopcroft, P. O., Lettenmaier, D. P.,  
665 Riley, W. J., Singarayer, J. S., Subin, Z. M., Tian, H., Zurcher, S., Brovkin, V., van Bodegom, P.  
666 M., Kleinen, T., Yu, Z. C., and Kaplan, J. O.: Present state of global wetland extent and  
667 wetland methane modelling: conclusions from a model inter-comparison project  
668 (WETCHIMP), *Biogeosciences*, 10, 753-788, 10.5194/bg-10-753-2013, 2013.  
669 Morton, D. C., Nagol, J., Carabajal, C. C., Rosette, J., Palace, M., Cook, B. D., Vermote, E. F.,  
670 Harding, D. J., and North, P. R. J.: Amazon forests maintain consistent canopy structure and  
671 greenness during the dry season, *Nature*, 506, 221-224, 10.1038/nature13006  
672 [http://www.nature.com/nature/journal/v506/n7487/abs/nature13006.html - supplementary-](http://www.nature.com/nature/journal/v506/n7487/abs/nature13006.html)  
673 [information](#), 2014.



674 Nisbet, E. G., Dlugokencky, E. J., and Bousquet, P.: Methane on the Rise—Again, *Science*,  
675 343, 493-495, 10.1126/science.1247828, 2014.

676 Saikawa, E., Schlosser, C. A., and Prinn, R. G.: Global modeling of soil nitrous oxide emissions  
677 from natural processes, *Global Biogeochemical Cycles*, 27, 972-989, 10.1002/gbc.20087,  
678 2013.

679 Saikawa, E., Prinn, R. G., Dlugokencky, E., Ishijima, K., Dutton, G. S., Hall, B. D., Langenfelds,  
680 R., Tohjima, Y., Machida, T., Manizza, M., Rigby, M., O'Doherty, S., Patra, P. K., Harth, C. M.,  
681 Weiss, R. F., Krummel, P. B., van der Schoot, M., Fraser, P. J., Steele, L. P., Aoki, S.,  
682 Nakazawa, T., and Elkins, J. W.: Global and regional emissions estimates for N<sub>2</sub>O,  
683 *Atmospheric Chemistry and Physics*, 14, 4617-4641, 10.5194/acp-14-4617-2014, 2014.

684 Saleska, S. R., Wu, J., Guan, K., Araujo, A. C., Huete, A., Nobre, A. D., and Restrepo-Coupe,  
685 N.: Dry-season greening of Amazon forests, *Nature*, 531, E4-E5, 10.1038/nature16457, 2016.

686 Schlesinger, W. H.: An estimate of the global sink for nitrous oxide in soils, *Global Change  
687 Biology*, 19, 2929-2931, 10.1111/gcb.12239, 2013.

688 Schulman, L., Ruokolainen, K., and Tuomisto, H.: Parameters for global ecosystem models,  
689 *Nature*, 399, 535-536, 1999.

690 Sjögersten, S., Black, C. R., Evers, S., Hoyos-Santillan, J., Wright, E. L., and Turner, B. L.:  
691 Tropical wetlands: A missing link in the global carbon cycle?, *Global Biogeochemical Cycles*,  
692 28, 1371-1386, 10.1002/2014GB004844, 2014.

693 Smith, L. K., Lewis, W. M., Chanton, J. P., Cronin, G., and Hamilton, S. K.: Methane emissions  
694 from the Orinoco River floodplain, Venezuela., *Biogeochemistry*, 51, 113-140, 2000.

695 Teh, Y. A., Silver, W. L., and Conrad, M. E.: Oxygen effects on methane production and  
696 oxidation in humid tropical forest soils, *Global Change Biology*, 11, 1283-1297,  
697 10.1111/j.1365-2486.2005.00983.x, 2005.



698 Teh, Y. A., Diem, T., Jones, S., Huaraca Quispe, L. P., Baggs, E., Morley, N., Richards, M.,  
699 Smith, P., and Meir, P.: Methane and nitrous oxide fluxes across an elevation gradient in the  
700 tropical Peruvian Andes, *Biogeosciences*, 11, 2325-2339, 10.5194/bg-11-2325-2014, 2014.  
701 Wen, Y., Chen, Z., Dannenmann, M., Carminati, A., Willibald, G., Kiese, R., Wolf, B.,  
702 Veldkamp, E., Butterbach-Bahl, K., and Corre, M. D.: Disentangling gross N<sub>2</sub>O production  
703 and consumption in soil, *Sci Rep*, 6, 8, 10.1038/srep36517, 2016.  
704 Werner, C., Butterbach-Bahl, K., Haas, E., Hickler, T., and Kiese, R.: A global inventory of N<sub>2</sub>O  
705 emissions from tropical rainforest soils using a detailed biogeochemical model, *Global  
706 Biogeochemical Cycles*, 21, 1-18, Gb3010  
707 10.1029/2006gb002909, 2007.  
708 Whiting, G. J., and Chanton, J. P.: Primary production control of methane emission from  
709 wetlands., *Nature*, 364, 794-795, 1993.  
710 Wilson, C., Gloor, M., Gatti, L. V., Miller, J. B., Monks, S. A., McNorton, J., Bloom, A. A.,  
711 Basso, L. S., and Chipperfield, M. P.: Contribution of regional sources to atmospheric  
712 methane over the Amazon Basin in 2010 and 2011, *Global Biogeochem. Cycles*, 30, 400–420,  
713 10.1002/2015GB005300, 2016.  
714 Yang, W. H., Teh, Y. A., and Silver, W. L.: A test of a field-based N-15-nitrous oxide pool  
715 dilution technique to measure gross N<sub>2</sub>O production in soil, *Global Change Biology*, 17,  
716 3577-3588, 10.1111/j.1365-2486.2011.02481.x, 2011.  
717 Ye, R., and Horwath, W. R.: Nitrous oxide uptake in rewetted wetlands with contrasting soil  
718 organic carbon contents, *Soil Biology and Biochemistry*, 100, 110-117,  
719 <http://dx.doi.org/10.1016/j.soilbio.2016.06.009>, 2016.



720 **11. TABLES AND FIGURES**

721 **Table 1.** Site characteristics including field site location, nutrient status, plot and flux chamber

722 replication

Vegetation type	Site name	Nutrient status*	Latitude (S)	Longitude (W)	Plots	Flux chambers
Forested	Buena Vista	Rich	4°14'45.60"S	73°12'0.20"W	9	74
Forested (short pole)	San Jorge (centre)	Poor	4°03'35.95"S	73°12'01.13"W	3	26
Forested (short pole)	Miraflores	Poor	4°28'16.59"S	74° 4'39.95"W	16	142
M. flexuosa Palm Swamp	Quistococha	Intermediate	3°49'57.61"S	73°12'01.13"W	119	433
M. flexuosa Palm Swamp	San Jorge (edge)	Intermediate	4°03'18.83"S	73°10'16.80"W	6	81
Mixed palm swamp	Charo	Rich	4°16'21.80"S	73°15'27.80"W	8	56

723 \*After Householder et al. 2012, Lahteenoja et al. 2009a, and Lahteenoja et al. 2009b



725 **Table 2.** Environmental variables for each vegetation type for the wet and dry season.

726 Values reported here are means and standard errors. Lower case letters indicate significant  
727 differences among vegetation types within the wet or dry season (Fisher's LSD,  $P < 0.05$ ).

728

Vegetation Type	Peat Temperature (°C)		Air Temperature (°C)		Conductivity (µS m⁻²)		Dissolved Oxygen (%)		Water Table Level (cm)		pH	
	Wet Season	Dry Season	Wet Season	Dry Season	Wet Season	Dry Season	Wet Season	Dry Season	Wet Season	Dry Season	Wet Season	Dry Season
Forested	26.1 ± 0.1a	24.7 ± 0.0a	28.8 ± 0.7a	26.4 ± 0.3a	79.0 ± 5.9a	75.9 ± 5.7a	0.2 ± 0.1a	18.9 ± 4.4a	110.8 ± 9.3a	-13.2 ± 0.7a	5.88 ± 0.15a	6.31 ± 0.04a
Forested (short pole)	25.2 ± 0.0b	24.8 ± 0.1a	27.6 ± 0.1b	27.5 ± 0.1b	21.0 ± 0.0b	48.5 ± 4.8b	4.4 ± 0.0a	33.1 ± 2.6b	26.9 ± 0.5b	-4.7 ± 0.4b	4.88 ± 0.01b	3.8 ± 0.03b
<i>M. flexuosa</i>	25.6 ± 0.6c	25.3 ± 0.1b	26.3 ± 0.1c	26.4 ± 0.1a	45.9 ± 2.1c	51.9 ± 1.8b	19.4 ± 1.3b	17.3 ± 1.5a	37.2 ± 1.7c	6.1 ± 1.3c	5.04 ± 0.03c	5.49 ± 0.03c
Mixed Palm Swamp	26.0 ± 0.0a	25.0 ± 0.1ab	26.1 ± 0.1c	28.2 ± 0.3b	100.0 ± 0.2d	206.4 ± 4.2c	0.0 ± 0.0a	0.0 ± 0.0c	183.7 ± 1.7d	-2.4 ± 1.7d	6.1 ± 0.3b	6.82 ± 0.03a



729 **Table 3.** Trace gas fluxes for each vegetation type for the wet and dry season. Values reported  
730 here are means and standard errors. Upper case letters indicate significant differences in gas  
731 flux between seasons with a vegetation type, while lower case letters indicate significant  
732 differences among vegetation types within a season (Fisher's LSD,  $P < 0.05$ ).

Vegetation Type	Methane Flux (mg CH <sub>4</sub> -C m <sup>-2</sup> d <sup>-1</sup> )		Nitrous Oxide Flux ( $\mu$ g N <sub>2</sub> O-N m <sup>-2</sup> d <sup>-1</sup> )	
	Wet Season	Dry Season	Wet Season	Dry Season
Forested	6.7 ± 1.0Aa	47.2 ± 5.4Ba	2.54 ± 1.48	-1.16 ± 1.20
Forested (short pole)	60.4 ± 9.1Ab	18.8 ± 2.6Bb	1.16 ± 0.54	-0.42 ± 0.90
<i>M. flexuosa</i> Palm Swamp	46.7 ± 8.4Ac	28.3 ± 2.6Bc	1.14 ± 0.35	0.92 ± 0.61
Mixed Palm Swamp	6.1 ± 1.3Aa	64.2 ± 12.1Ba	1.45 ± 0.79	-0.80 ± 0.79

733



734 **Figure Captions**

735 **Figure 1.** Map of the study region and field sites.

736

737 **Figure 2.** Net **(a)** CH<sub>4</sub> and **(b)** N<sub>2</sub>O fluxes by vegetation type. Boxes enclose the interquartile  
738 range, whiskers indicate the 90th and 10th percentiles. The solid line in each box represents  
739 the median. Individual points represent potential outliers.

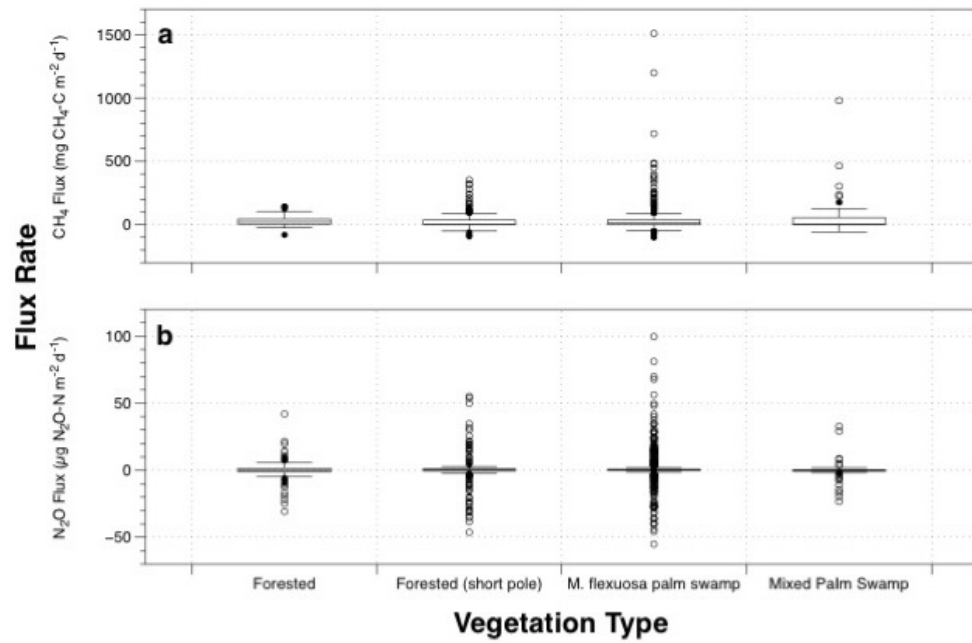


740 **Figure 1**





741 **Figure 2**



742